**Astronomy**
**&**
**Astrophysics**

# Helioseismic evidence of two solar granulation timescales

H. Vázquez Ramió[1], C. Régulo[1,2], and T. Roca Cortés[1,2]

[1] Instituto de Astrofísica de Canarias, 38200 La Laguna (Tenerife), Spain
  e-mail: hvr@iac.es
[2] Dpto. de Astrofísica, Universidad de La Laguna, 38206 La Laguna (Tenerife), Spain
  e-mail: crr@iac.es,trc@iac.es

**ABSTRACT**

The signature of two different scales of solar granulation in the power spectrum of disk integrated irradiance time series is presented. The fitted timescales for granulation ($\tau_{GR1} \approx 237$ s and $\tau_{GR2} \approx 62$ s) are in good agreement with the characteristic lifetimes derived from recent image time series of the Sun's surface (Del Moro 2004); and probably linked to magnetic chromospheric structures such as bright points (Harvey et al. 1993).

**Key words.** Sun: helioseismology – Sun: photosphere – Sun: granulation – Sun: activity

## 1. Introduction

It is well known that time evolution of solar surface inhomogeneities such as convection structures and sunspots leave a signature in the background of its acoustic power spectrum which is usually modeled by a function proposed by Harvey (Harvey 1984; Harvey et al. 1993). This assumes that the time evolution of the autocovariance function of a particular scale of solar convection (i.e. granulation, supergranulation, etc.) follows an exponential decay. This model had been used to fit the power spectra both from irradiance and from velocity observed time series, although depending on the type of signal and on the wavelength observed the detected convection structures may change; for instance, the mesogranulation is observed in velocity but not in irradiance (Régulo et al. 2002; Vázquez Ramió et al. 2002).

In this work it is shown that, when analyzing irradiance data from Variability of solar IRradiance and Gravity Oscillations (VIRGO) instrument, on board the SOlar and Heliospheric Observatory (SOHO) mission, three convection structures (with different characteristic timescales and rms amplitudes) are detected: granulation, supergranulation, and a third component close to the granulation one which is necessary to fit to the data better. A similar component was attributed by Harvey et al. (1993) to chromospheric bright points. Furthermore recent observations of three different time series of solar surface images by Del Moro (2004) suggested that granulation has two predominant populations: one with lifetimes of 3–4 min and another with 1 min.

In Sects. 2 and 3 the observations and methodology of data analysis is presented while in Sect. 4 the results are given and discussed.

## 2. Observations

Observational data consist of disk integrated solar irradiance time series obtained from the 3-channel Sun photometer (SPM) of VIRGO experiment on board SOHO. Data is simultaneously obtained at three wavelengths: 402 nm (blue), 500 nm (green) and 865 nm (red) at a cadence of 60 s. Two sets of data series corresponding to periods of minimum (from 11th April, 1996 to 3rd August, 1997) and maximum activity (from 1st March, 2000 to 23rd June, 2001) were taken to get the associated spectra. Level 1 data from Virgo Data Center, at *Instituto de Astrofísica de Canarias* (*IAC*), were collected and then detrended for ageing by fitting a second order polynomial to the log of the photometric counts. The final analyzed series is the result of averaging 5 spectra associated to subseries of 96 days each, in order to make the power spectrum smoother. Fast Fourier Transform (FFT) techniques were employed.

## 3. Analysis

Solar convective spectral power is present from the region of p-modes (at $\nu \sim 3$ mHz) to lower frequencies and its nature is non-periodic. In that regard, a local average into a uniform logarithmic grid in frequency makes the power distribution smoother and the fitting of the model easier along the frequency axis. This procedure reduces the number of original bins of the spectrum by a factor of about 200, yielding finally 149 frequency bins. The variances $\sigma^2$ of each average were employed as the fitting weights ($1/\sigma^2$).

Considering the nature of the solar convection structures signal, the background of the global oscillation power spectrum was modeled as the total contribution of structures represented

by functions with two parameters each: the characteristic timescale of the phenomenon ($\tau$) and another related with the rms amplitude ($A$). So that the function to fit the power spectrum is one of this type:

$$P(\nu) = \sum_{i=0}^{N} \frac{A_i}{1 + (2\pi\nu\tau_i)^2}, \qquad (1)$$

where $P$ is the spectral power, $\nu$ is the frequency and the index $i$ refers to the $i$th of the $N$ convective features to fit. This simple model provides a good and robust estimation of the timescales of convective components. This study is focused on the granulation, so the fit is constrained to the frequency range $\nu \in (10^{-5}, 2.5 \times 10^{-3})$ Hz i.e., from the region of the spectrum where long-period structures (such as supergranulation) dominate the power to frequencies where the contribution of the p-modes is negligible.

A long-period component with $\tau$ from $10^4$ s to $10^5$ s, which corresponds to supergranulation, was included to reproduce the shape of the spectral power at low frequencies, just below granulation. It must be taken into account that the frequency range that we fit is not wide enough to derive parameters for supergranulation; this is out of the scope of this work. Two different models were fit to the spectra, one with an additional component of the type of Eq. (1) for granulation (so, with $N = 2$) and another with two components of granulation ($N = 3$).

The fits were performed employing the grid-search non-linear least-squares method (Bevington & Robinson 2003). The set of initial values were selected in such a way that the area under the model was approximately the same as that under the observed power spectrum. The goodness of the fit was evaluated through the reduced $\chi^2$ function (normalized by the number of degrees of freedom $f = N_{\text{bins}} - N_{\text{par}}$, being $N_{\text{bins}}$ the number of bins employed in the fit and $N_{\text{par}}$ the number of parameters used in the model).

$$\chi_f^2 = \frac{1}{f} \cdot \sum_{k=1}^{N_{\text{bins}}} \frac{[P_k - P(\nu_k)]^2}{\sigma_k^2} \qquad (2)$$

$P(\nu_k)$ is the modeled spectral power at the $k$th bin, $P_k$ the corresponding observed one and $\sigma_k^2$ the associated variance of the mean due to the gridding process. Slight shifts from the starting guess values gave rise to practically the same results, while significant variations of them were needed to change the results of the fit. Different trials of the initial guesses were performed to find the fit that yielded the lowest $\chi_f^2$.

In order to study whether one or two components for granulation are needed to provide a better fit, we compared the results obtained from the model with only one structure for granulation ($\chi_{f_1}^2$) with the one with two granulation scales ($\chi_{f_2}^2$), evaluating the Fisher's distribution $\wp_F(F_{1,2} = \chi_{f_1}^2/\chi_{f_2}^2; f_1, f_2)$ (Bevington & Robinson 2003). We are, in fact, interested in the integral probability $P_F(F_{1,2}, f_1, f_2)$ defined as:

$$P_F(F_{1,2}, f_1, f_2) = \int_{F_{1,2}}^{\infty} \wp_F(F_{1,2}; f_1, f_2) \cdot \mathrm{d}F. \qquad (3)$$

This value describes the probability of observing a given ratio $F_{1,2} = \chi_{f_1}^2/\chi_{f_2}^2$ or greater from a random set of data when compared to the correct fitting function.

Since the difference between both kind of fits, in the present study, is the inclusion or not of two new parameters in the model, the ratio $F_\chi$ defined as:

$$F_\chi = \frac{\left[\chi^2(f_1) - \chi^2(f_2)\right]/(f_1 - f_2)}{\chi_{f_2}^2} \qquad (4)$$

where $\chi^2(f_i) = \chi_{f_i}^2 \cdot f_i$ for $i = 1, 2$, is of particular interest because it can be used to test the reliability of the addition of new terms in the fitting function.

Due to the properties of chi-squared distributions, the observed value of $F_\chi$ is equivalent to a $F_{f_1-f_2,f_2}$ and hence should follow the $\wp_F(F_{f_1-f_2,f_2}; f_1 - f_2, f_2)$ distribution. Thus, by evaluating the probability corresponding to the observed value of $F_\chi$, one can determine whether the additional terms were needed or not. In our case $f_1 - f_2 = 2$, so values of $P_F(F_\chi, 2, f_2) \gtrsim 0.1$ should indicate that the new parameters do not really improve the fit (i.e. they are actually equal zero). On the other hand, lower values of $P_F(F_\chi, 2, f_2)$ (say less than 0.001) will mean that a significant improvement was achieved since the probability of obtaining similar or higher ratios $F_\chi$ is less than 0.1%, according to the Fisher's distribution.

## 4. Results and discussion

As mentioned in the preceding section, two types of models were used to fit to the spectra. One with only one structure for granulation and another with two structures. The timescales fitted in each case, depending on solar activity phase, observed bandwidth and number of fitted structures, are shown in Table 1, as well as the ratio $F_\chi$ defined above.

First of all, a test for the suitability of the introduction of the new component (two new parameters) in the fitting function was performed. We want to know if the differences in the $\chi^2$ resulting from the fits are probable or not. In all cases, $f_1 = 145$ and $f_2 = 143$, and the value of $F_{2,f_2}$ that yields a probability of 0.1%, i.e. $P_F(F_0; 2, f_2) = 0.001$, is $F_0 = 7.25$; we take $F_0$ as a test value. A value $F_\chi \gg F_0$ indicates that the additional structure, modeled with two additional parameters, is reliable. The improvement of the fit can be seen in Fig. 1, where the product $\nu \cdot P$ versus $\nu$ is plotted; such representation shows the non-periodic structures better than the usual $P$ versus $\nu$.

When fitting a unique structure for granulation (GR) the timescales are in the range from $\tau_{\text{GR}} = 194$ s to $\tau_{\text{GR}} = 212$ s, thus from 3.2 min to 3.5 min. These timescales are always shorter than the ones fitted as the first granulation structure (GR1) when two are included in the model: from $\tau_{\text{GR1}} = 218$ s to $\tau_{\text{GR1}} = 266$ s, while the second structure (GR2) has timescales from $\tau_{\text{GR2}} = 52$s to $\tau_{\text{GR2}} = 70$ s. This low value of $\tau_{\text{GR}}$, compared to $\tau_{\text{GR1}}$, can also be seen in Pallé et al. (1999), where a unique component (GR) was included in the fitting model to VIRGO data, yielding a mean value of $\tau_{\text{GR}} = 209$ s.

It is not clear from the results of the fits that there exists a change in the timescales of granulation with the activity cycle. The average values shown in Table 1 do not suggest any variation from minimum to maximum solar activity, which is in good agreement with previous observations (Vázquez Ramió et al. 2002).
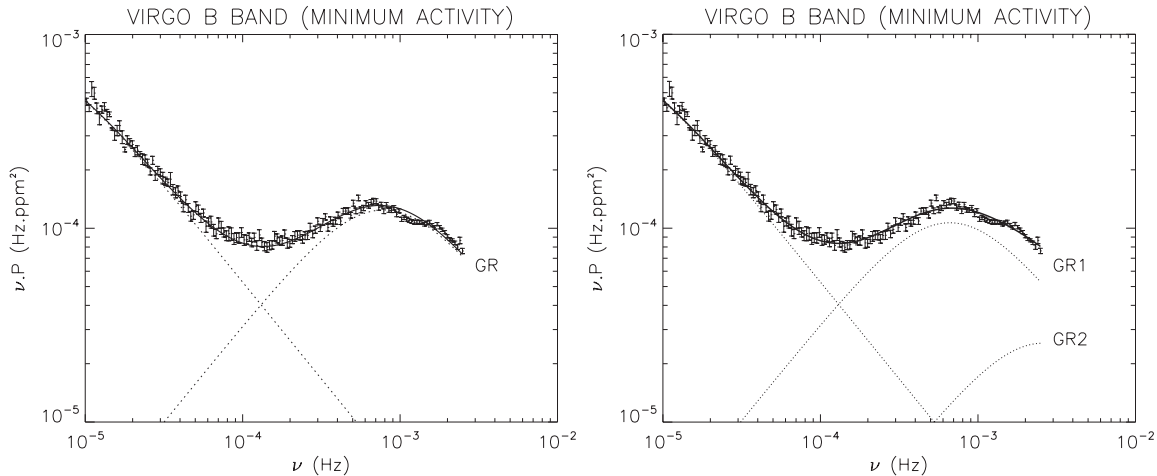
**Fig. 1.** Two of the fits of the irradiance background power spectra, corresponding to the *B* band during the phase of minimum solar activity. The plots employ a model with only one structure for granulation (*left*) and two structures (*right*). Each power spectrum was derived from a 480 days long series (5 × 96 days).

**Table 1.** Timescales of the model used to fit the background of the solar power spectra from VIRGO, at periods of maximum (MAX) and minimum (MIN) activity for the three wavelength bands. The granulation timescale in the case that only one structure is fitted is labelled as GR, while when two structures are fitted they are labelled as GR1 (slow) and GR2 (fast) granulation timescales. The calculated $F_\chi$ of each fit are also shown; values of $F_\chi > 7.25$ have a probability of less than 0.1%, indicating the reliability of the addition of GR2.

| MIN | $\tau_{GR}$ (s) | $\tau_{GR1}$ (s) | $\tau_{GR2}$ (s) | $F_\chi$ |
|---|---|---|---|---|
| B (402 nm) | 201.2 ± 0.5 | 240.5 ± 0.8 | 61.3 ± 1.7 | 32.5 |
| G (500 nm) | 193.5 ± 0.5 | 225.8 ± 0.7 | 66.8 ± 1.8 | 15.4 |
| R (865 nm) | 208.7 ± 0.6 | 266.0 ± 0.9 | 51.8 ± 1.1 | 64.4 |
| AVERAGE | 200.3 ± 4.2 | 240.8 ± 11 | 57.1 ± 4.4 | 37.4 |
| MAX | $\tau_{GR}$ (s) | $\tau_{GR1}$ (s) | $\tau_{GR2}$ (s) | $F_\chi$ |
| B (402 nm) | 191.2 ± 0.5 | 218.3 ± 0.7 | 69.6 ± 2.0 | 11.0 |
| G (500 nm) | 197.0 ± 0.5 | 230.5 ± 0.7 | 66.9 ± 1.7 | 16.9 |
| R (865 nm) | 212.4 ± 0.6 | 255.6 ± 0.8 | 64.8 ± 1.5 | 31.5 |
| AVERAGE | 198.8 ± 5.9 | 233.0 ± 11 | 66.7 ± 1.3 | 19.8 |

On the contrary, a dependency of granulation timescale $\tau_{GR1}$ with color (with atmospheric depth) could exist. Indeed, the timescales are observed to increase (see Table 1) with increasing wavelength. The SPM filter response functions have maximum contribution at geometrical heights $h$ above $\tau_{\lambda=500\,nm} = 1$: B ($h = -30$ km), G ($h = -15$ km) and R ($h = 10$ km) (Jiménez et al. 2005), but they are wide enough (∼200 km) to just distinguish some effect between B and G from R results. Further, numerical simulations of convection structures (Gadun et al. 2000) indicate that larger granular cells, which imply longer lifetimes (Title et al. 1989), cool down at higher heights, agreeing with our observed trend.

The inclusion of the second component (GR2) in the fitting model is not new. Harvey et al. (1993) found it necessary to include in order to fit the overall background spectrum from 17 days of observation of full solar disk in Ca II K-line from the South Pole. They used a model that included two periodic components attributed to a photospheric and a chromospheric oscillation, and a slightly different parameterization of the

non-periodic structures that left the power of the second term in the denominator of Eq. (1) as a free parameter. The fitted timescale was 84 s = 1.4 min and it was attributed to the evolution of the non-periodic fluctuations of chromospheric bright points. Additionally, the fitted granulation component had timescales of 220 s = 3.7 min.

In recent work by Vázquez Ramió et al. (2002) the same VIRGO spectra used in this work were analyzed to fit the whole background but including the periodic photospheric component and again, the model employed by Harvey et al. (1993) for non-periodic components, with the power in the denominator of Eq. (1) left free. To be able to fit the photospheric periodic component just mentioned, it was necessary to add an additional non-periodic component to the model, otherwise the fit did not converge properly. That *extra* component fitted had characteristic times of $\tau \approx 71$ s and it was suggested that it could be part of granulation. Although more sofisticated, that model including more free parameters than Eq. (1) does not give additional information neither on the number of convective structures to fit nor in the physical parameters involved. Moreover, the fits with such models are far less robust and do not provide significantly different results regarding the fitted timescales.

More recent observations consisting of time series of high resolution images of the quiet granulation at the solar disk centre, acquired with three different telescopes and instruments, were analyzed by Del Moro (2004). He suggested that at least two different granular populations were present: a bulk with a mean lifetime of 1 min and a minority with a longer mean lifetime of 3 min to 4 min. All these results are summarized in Table 2. As it can be seen, there is good agreement of both sets of timescales observed and published, $\tau_{GR1}$ and $\tau_{GR2}$, with the observations of Del Moro (2004) and they are consistent with the existence of at least, two populations of granulation with timescales of $\tau_{GR1}$ from 3.6 min to 4.4 min and $\tau_{GR2}$ from 0.9 min to 1.2 min.

This (GR2) component does not seem to be needed when dealing with velocity data; actually the studies in this sense do

**Table 2.** Fitted and published timescales when two structures (GR1) and (GR2) of the solar background power spectrum are included in the model. The references shown are: H1993: Harvey et al. (1993) and VR2002: Vázquez Ramió et al. (2002), both from full-disk observations; and DM2004: Del Moro (2004) (three different time series of high resolution images). The last six results are the ones obtained from the present study. The epoch (years form '88 to '01) when each data were acquired and the central wavelength observed are also shown, as well as the phase of the solar magnetic activity (MIN/MAX).

| | $\lambda_0$ (nm) | EPOCH | $\tau_{GR1}$ (s) | $\tau_{GR2}$ (s) |
|---|---|---|---|---|
| H1993 | 393.3 | 88 | 220 | 84 |
| VR2002 B [MIN] | 402 | 96–97 | 207.5 ± 13 | 79 ± 8 |
| VR2002 G [MIN] | 500 | 96–97 | 223.4 ± 42 | 67 ± 30 |
| VR2002 R [MIN] | 865 | 96–97 | 258.0 ± 63 | 72 ± 40 |
| VR2002 B [MAX] | 402 | 00–01 | 219.9 ± 52 | 71 ± 28 |
| VR2002 G [MAX] | 500 | 00–01 | 239.2 ± 56 | 69 ± 30 |
| VR2002 R [MAX] | 865 | 00–01 | 243.6 ± 42 | 68 ± 23 |
| DM2004[A] | 525.7 | 95 | 246 ± 12 | 78.0 ± 3 |
| DM2004[B] | 550.0 | 96 | 162 ± 6 | 60.0 ± 1.2 |
| DM2004[C] | 538.0 | 99 | 156 ± 6 | 54.0 ± 1.2 |
| B [MIN] | 402 | 96–97 | 240.5 ± 0.8 | 61.3 ± 1.7 |
| G [MIN] | 500 | 96–97 | 225.8 ± 0.7 | 66.8 ± 1.8 |
| R [MIN] | 865 | 96–97 | 266.0 ± 0.9 | 51.8 ± 1.1 |
| B [MAX] | 402 | 00–01 | 218.3 ± 0.7 | 69.6 ± 2.0 |
| G [MAX] | 500 | 00–01 | 230.5 ± 0.7 | 66.9 ± 1.7 |
| R [MAX] | 865 | 00–01 | 255.6 ± 0.8 | 64.8 ± 1.5 |

not include it in the fittings (Pallé et al. 1999; Régulo et al. 2002). Moreover, the timescales of a unique granulation component (GR) fitted in velocity are larger ($\tau_{GR} > 400$ s) than the same fitted in irradiance $\tau_{GR} < 220$ s (although the differences are smaller if we accept that two components are observed in irradiance and we compare $\tau_{GR}$ from velocity with $\tau_{GR1} < 270$ s). This means that the same granulation phenomenon is observed quite different in irradiance and in velocity; changes of contrast can be only observed when a certain amount of temperature fluctuations happen, so changes in the velocity fields might occur not yielding a significant variation in irradiance. This could also explain the fact that the so-called chromospheric oscillation is observed in velocity but not in all wavelengths in irradiance. The detection of the mesogranulation component in velocity and not in irradiance should indicate that again, this component does not involve temperature variations observable through irradiance fluctuations.

## 5. Conclusions

A simple model with non-periodic solar convective components has been used to fit the background power spectrum from VIRGO irradiance data at low and high phases of solar activity. Two kind of models were employed, one with only one granulation component and another with two. The fits were performed in the frequency range from $\nu = 10^{-5}$ Hz to $\nu = 2.5 \times 10^{-3}$ Hz, focusing on granulation signal.

The suitability of the addition of the new structure (GR2) in the fitting model was checked through the F-test, which involves the evaluation of the ratio of chisquares $F_\chi$ and the Fisher's probability distribution. In all cases, the observed $F_\chi$ exceeds by far the test value. This implies that the new parameters are reliable in the model, because they do significantly improve the fit.

The inclusion of this new component (GR2 with $\tau_{GR2} \approx 62$ s) yields an increase of about 15%–20% on the timescale $\tau_{GR1} \approx 237$ s when compared to the one fitted with only one component for granulation $\tau_{GR} \approx 200$ s, which is consistent with the values of $\tau_{GR}$ found by Pallé et al. (1999). Moreover, an increase of the longest timescale $\tau_{GR1}$ with wavelength is observed, but no significant variations of both, $\tau_{GR1}$ and $\tau_{GR2}$, are found from maximum to minimum solar activity, as also remarked in Vázquez Ramió et al. (2002).

The recent observations by Del Moro (2004) of regions of quiet solar granulation acquiring high resolution images time series suggested that, at least, two granular populations with different characteristic times coexist. Results found here also support these findings and represent a helioseismic evidence of the existence of two granulation timescales. If Harvey et al. (1993) are correct in assigning their short-lived component to bright points (chromospheric magnetic structures) then we could think that both observations are part of the same phenomenon. This small scale granulation could drive the magnetic fields that would yield the chromospheric bright points.

## References

Bevington, P. R., & Robinson, D. K. 2003, Data Reduction and Error Analysis for the Physical Sciences, 3rd ed. (McGraw-Hill)
Del Moro, D. 2004, A&A, 428, 1007
Fröhlich, C., Romero, J., Roth, H., et al. 1995, Sol. Phys., 162, 101
Gadun, A. S., Hanslmeier, A., Pikalov, K. N., et al. 2000, A&AS, 146, 267
Harvey, J. W. 1984, in Probing the Depths of a Star: The Study of the Solar Oscillation from the Space, ed. R. W. Noyes & E. J. Rhodes Jr., Pasadena, JPL/NASA, 327, 51
Harvey, J. W., Duvall T. L., Jr., Jefferies, S. M., & Pomerantz, M. A. 1993, ASP Conf. Ser., 42, 111
Jiménez, A., Jiménez-Reyes, S. J., & García, R. A. 2005, ApJ, 623, 1215
Pallé, P. L., Roca Cortés, T., Jiménez, A., GOLF & VIRGO Teams 1999, ASP Conf. Ser., 173, 297
Régulo, C., Roca Cortés, T., & Vázquez Ramió, H. 2002, ESA SP-506, 2, 889
Title, A. M., Tarbell, T. D., Topka, K. P., Ferguson, S. H., Shine, R. A., & SOUP Team 1989, ApJ, 336, 475
Vázquez Ramió, H., Roca Cortés, T., & Régulo, C. 2002, ESA SP-506, 2, 897